Exergy analysis of cold recovery in a cryogenic packed bed system

Chamarthi Bharat Surya, Pavitra Sandilya

Cryogenic Engineering Centre, Indian Institute of Technology Kharagpur, Kharagpur, 721302, West Bengal, India
E-mail ID: profsandilya@gmail.com

Cold recovery and storage in a packed bed is suggested during the regasification of LNG and liquefied air; the latter is found in a cryogenic energy storage system. The efficiency of cold recovery depends on the pressure, temperature, thermophysical properties of the packing material and the fluid, fluid flow rate, bed geometry and bed dimension. These factors dictate the irreversibilities accompanying the heat leakage from the surroundings, heat transfer between the flowing cryogen and the packing material and pressure drop along the flow direction. These irreversibilities lead to exergy losses in the packed bed. As a result, the exergy efficiency of the charging operation is lowered. The present work focuses on the effect of inlet temperature on the thermodynamic performance of cryogenic packed bed during charging. Losses due to irreversibilities are quantified and exergy efficiency of charging operation is evaluated. It was seen that the axial conduction within the bed resulted in temperature drop at the outlet, thereby reducing the exergy efficiency of the charging operation. The exergy efficiency of the charging operation increased with inlet temperatures.

1. INTRODUCTION

Sensible heat-based packed bed thermal energy storage systems have been studied for energy storage applications, especially for solar energy. In a packed bed system, thermal energy is stored in times of excess power, and is later used for power production in times of demand. In similar lines, a vast source of cold thermal energy at cryogenic temperatures may be recovered using packed beds at LNG regasification sites and Liquid Air Energy Storage (LAES) plants. Cold energy at these sites can be stored and reused for wide range of applications requiring varying levels of refrigeration and power. Cold storage in a packed bed happens in three stages - charging, standby and discharging. During the charging stage, cold energy from the site is transferred by a working fluid such as air to a packed bed. The packing material may be a rock, plastic which store sensible heat or a Phase Change Material (PCM) which store energy as both sensible and a latent heat. The cold is then retained by the bed during a standby or idle stage until the discharging stage, during which the stored cold energy is taken up by a working fluid from the bed and transferred to the application site. Initial conceptualization of using packed bed in cryogenic energy storage was put forward by Smith [1]. A regenerator made of stainless-steel porous matrix was proposed for regasifying liquid cryogen. The first pilot scale demonstration of LAES plant at Birmingham [2] used packed bed cryogenic storage systems to recover the cold released during the regasification stage of a LAES pilot plant. The recovered cold was further used to provide refrigeration for liquefaction cycle of LAES. 51% of the cold energy generated during regasification stage was recycled using

packed bed system. Later on, thermodynamic performance studies on LAES with packed bed systems showed thermal degradation within the bed lead to reduction in refrigeration available for liquefaction [3].

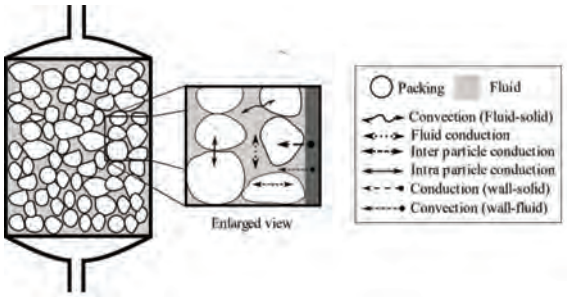

Figure 1. Heat transfer mechanisms in a packed bed

Figure 1 shows various heat transfer mechanisms involved in storage and degradation of energy in a packed bed cryogenic system. Convection between the working fluid and the packing material is the dominant heat transfer mechanism during charging and discharging operations. During standby or idle period where no flow takes place, conduction in the axial/radial direction will result in self-discharge, which in turn reduces the cold storage efficiency [4].

Heat transfer interactions with the wall through conduction and convection result in heat inleaks, which may be minimised by careful design of the storage system and insulation and optimal choice of operating parameters such as inlet temperature, type of packing, mass flow rate, particle diameter etc. For instance, thermodynamic performance evaluation on cryogenic packed bed by Tan [5] showed that the cold storage efficiency decreased with temperature and particle diameter didn't bear a significant effect on charging performance. From the limited studies available in the open literature on thermodynamic performance of cryogenic packed beds, it is seen that the performance evaluation was confined to calculation of first or second law efficiency but the contribution of various loss mechanisms hasn't been reported under various operating parameters.

1.1 Objective

In this work, we aim to study the effect of inlet temperature on the exergy efficiency of charging operation in a packed bed.

To meet this objective, we considered a 1-dimensional model of charging process in a packed bed system to obtain the temperature and flow distribution in the bed. Using this information, we quantified the losses occurring during the operation to evaluate the exergy efficiency.

2. MODELLING

A 1-dimensional single-phase model has been developed in this study. Figure 2 shows the computational domain of the packed bed. Along with continuity and momentum, a single energy equation is solved for both the working fluid (nitrogen) and packing material (quartz) using finite volume based FLUENT module of the commercial software ANSYS 2019R3. An effective thermal conductivity is considered in the energy equation which accounts for various heat transfer interactions taking place in the bed.

Figure 2. Computational domain

The assumptions of this model are:

1. Conduction takes place only in the axial direction. The insulation considered is assumed to prevent any significant heat inleaks. Hence, no radial gradients will be setup in the bed.
2. The flow is incompressible and plug.
3. Axisymmetric flow and heat transfer phenomena.
4. Local thermal equilibrium is valid for the given fluid-packing material combination since the thermal conductivity and volumetric heat capacity of the packing is higher than the fluid.

The packing material has a sphericity

equal to one. The temperature dependent thermophysical properties of the working fluid (air) and packing material (quartz) were taken from NIST database [6] and Sciacovelli [3] respectively. The reported values were fitted as a function of temperature according to equation 1.

$$\psi = a_0 + a_1.T + a_2.T^2 + a_3.T^3 \quad ...(1)$$

The coefficient values of the equation 1 are given in Table 1.

In this model, a single energy equation is solved for both the phases. The resulting temperature distribution represents the bed temperature.

The continuity, momentum and energy equations solved are given in equations 2,3 and 4 respectively [5].

$$\frac{\partial \rho}{\partial t} + \frac{\partial}{\partial z}\left(\rho \frac{\partial u}{\partial z}\right) = 0 \quad ...(2)$$

$$\frac{\partial u}{\partial t} + u\frac{\partial u}{\partial z} = \frac{\partial p}{\partial z} + \frac{\partial}{\partial z}\left(\mu \frac{\partial u}{\partial z}\right) - \alpha.\mu.u. - \beta.\rho u.|u| \quad ...(3)$$

$$\left(\rho c_p\right)_{eff}\left(\frac{\partial T}{\partial t} + u.\frac{\partial T}{\partial z}\right) = \frac{\partial}{\partial z}\left(k_{eff}\frac{\partial T}{\partial z}\right) \quad ...(4)$$

The porous modelling is incorporated via momentum sink terms, i.e., the last two terms in the right-hand side of equation 3. These terms account for the additional pressure drop that the flow experiences due to the porous structure of the bed. The constants and (equation 6) are the coefficients of linear and quadratic terms of Ergun equation (equation 5) used for calculating pressure drop through a porous medium.

$$\frac{\Delta P}{L} = 150\frac{(1-\epsilon)^2}{\epsilon^3}\frac{\mu U_m}{d_p^2} + 1.75\frac{1-\epsilon}{\epsilon^3}\frac{G U_m}{d_p} \quad ...(5)$$

$$\text{Here, } \alpha = 150\frac{(1-\varepsilon)^2}{\varepsilon^3 d_p^2};\ \beta = \frac{1.75}{d_p}\frac{(1-\varepsilon)}{\varepsilon^3} \quad ...(6)$$

$$\varepsilon = 0.375 + 0.17.\frac{d_p}{D} + 0.39\left(\frac{d_p}{D}\right)^2 \quad ...(7)$$

In equation 4, the effective thermal conductivity (k_{eff}) of the bed in axial direction is estimated using equation 8.

$$k_{eff} = k_{still} + k_{flow} \quad ...(8)$$

In equation 8, k_{still} is the standstill thermal conductivity of the bed when heat transfer happens purely through conduction. k_{still} is estimated using correlation reported by Gonzo et al [7]. k_{flow} is the contribution of advection towards the effective thermal conductivity of the bed when flow takes place. k_{flow} is estimated using equation 9 [8].

$$k_{flow} = 0.5\, k_f \mathrm{Re}_p.\mathrm{Pr} \quad ...(9)$$

$\left(\rho c_p\right)_{eff}$ in equation 4 is estimated using a simple weighted average volumetric heat capacity of the fluid and packing according to equation 10.

$$\left(\rho c_p\right)_{eff} = \varepsilon\left(\rho c_p\right)_f + (1-\varepsilon)\left(\rho c_p\right)_s \quad ...(10)$$

The imposed boundary and initial conditions are shown in Table 2.

Table 1. Coefficient values of temperature dependent thermophysical properties of the packing and gas

	a_1	a_2	a_3
k_s	13.941	-0.0265	-
C_s	108.4	4.184	-0.0043
ρ_f	6.8195	-0.029	4×10^{-5}
$c_{p,f}$	1074	-0.2554	0.0004
μ_f	3×10^{-6}	5×10^{-8}	-
k_f	0.0014	8×10^{-5}	-

Table 2. Initial and boundary conditions

Initial Conditions	
Bed	$T = T_{bed}\ \forall\ z$
Insulation	$T = T_{bed}\ \forall\ z$
Boundary conditions	
$z = 0$	$u = U_s;\ T = T_c$
$z = L$	$P = P_{atm}$
$r = R$	$u = 0$
$r = 0$	$\frac{du}{dr} = 0; \frac{dT}{dr} = 0$

2.1 Exergy formulation

Irreversibilities in a packed bed system during charging operation exist in the form of:

1. Pressure drops
2. Axial Conduction
3. Outflow of cold gas

Each of these irreversibilities lead to exergy losses. As a result, the exergy associated with the cold fluid at the bed inlet is not completely stored in the bed. Equation 11 gives an exergy balance for charging operation.

Exergy balance during the charging operation is given by:

$$\dot{\gamma}_{in} - \dot{\gamma}_{out} - \dot{\gamma}_{d,ch} = \frac{d(\gamma)_{st,bed}}{dt} \quad ...(11)$$

In equation 11, and represent the inlet and outlet exergy associated with the fluid and are determined from respectively. During charging, represents a loss is the stored exergy content of the bed

$$\dot{\gamma_{\text{in}}} = \dot{m_{\text{in}}}.[(h_{\text{in}} - h_{\text{ref}}) - T_{\text{ref}}(s_{\text{in}} - s_{\text{ref}})]t_{\text{ch}} \quad ...(12)$$

$$\dot{\gamma_{\text{out}}} = \dot{m_{\text{out}}}.[(h_{\text{out}} - h_{\text{ref}}) - T_{\text{ref}}(s_{\text{out}} - s_{\text{ref}})]t_{\text{ch}} \quad ...(13)$$

In equation 12 and 13, t_{ch} is duration of charging, h and s represent the specific enthalpy and entropy respectively. The subscript 'ref' refers to the reference(dead) state properties. The reference temperature was taken as the ambient temperature reported in Dutta's. experiments. at 306 K (T_{bed}).

The exergy destruction ($\gamma_{\text{d,ch}}$) within the bed is the sum of exergy loss due to pressure drop and axial conduction within the bed. These quantities can be related to the entropy generation rate ($\dot{S}_{\text{gen}}$) by Guoy-Stodola theorem according to equation 14.

$$\gamma_{\text{d,ch}} = T_{\text{ref}}.\dot{S}_{\text{gen}} \quad ...(14)$$

Equation 15 and 16 give the volumetric entropy generation rate due to axial conduction and pressure drop respectively [8].

$$\dot{S}_{\text{gen,c}} = \frac{1}{\text{T}^2}.\text{k}_{\text{eff}}.\left(\frac{\text{dT}}{\text{dz}}\right)^2 \quad ...(15)$$

$$\dot{S}_{\text{gen,p}} = \frac{\dot{\text{m}}}{\rho_{\text{f}}} Rln\left(\frac{P_{\text{in}}}{P_{\text{out}}}\right) \quad ...(16)$$

The exergy efficiency () of the charging operation is found using equation 17.

$$\phi = \frac{\gamma_{\text{st,bed}}}{\gamma_{\text{in}}} = 1 - \frac{\gamma_{\text{d,ch}} + \gamma_{\text{out}}}{\gamma_{\text{in}}} \quad ...(17)$$

3. RESULTS & DISCUSSION

Before proceeding with the parametric study, the model was checked for its grid convergence. The design and operating conditions for grid independence study are given in Table 3. Implicit transient formulation was employed with a time step size of 1 (one) second. Four grid sizes – 2.5 mm 5 mm, 10 mm and 20 mm were considered for this study. We monitored the maximum change in bed temperature with change in grid sizes at different times. Figure 3 shows the results of the gird independence study. The X-axis value ($H/\Delta z_c - \Delta z_f$) represents the change in number of cells between two consecutive grid sizes.

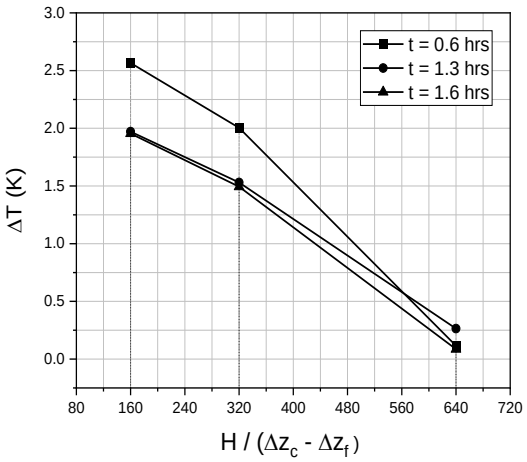

Figure 3. Grid independence study

It was seen that ΔT reduced as the grid sizes were reduced. The change in temperature (ΔT ~ 0.03 K) was practically indistinguishable between element sizes of 5 mm and 2.5mm ($H/\Delta z_c$ Δz_f = 640). Hence, a grid size of 5mm was chosen for the studies.

3.1 Model validation

Table 3 gives the parameters of the validation case taken from experimental studies reported by Dutta [1]. Figure 4 shows the transient temperature distribution at an axial distance of 0.26 m and 0.16m from the inlet obtained from current model and reported experimental data. The maximum deviation in the temperature reading was found to be 10%. This deviation may be attributed majorly to the following reasons:

1. Heat transfer in radial direction was not considered. This caused the temperature to drop much quickly during charging.
2. k_{eff} was estimated based on correlations reported using experiments at high temperatures (above ambient). This quantity caused a larger thermal dispersion during the start of charging.

Table 3. Geometry and operating parameters

Geometry and operating parameters	
Bed height (H)	0.32 m
Bed diameter (D)	0.15 m
Particle diameter (d_p)	11.25 mm
Insulation thickness (t)	0.1 m
Inlet temperature (T_{ch})	175 K
Initial bed temperature (T_{bed})	306 K
Inlet mass flux (G)	0.088 kg/m^{2}s
Inlet pressure (P_{in})	150 kPa
Packing material	Gravel (pebbles)
Bed voidage	0.38
Rock (average density)	2688 kg/m^3

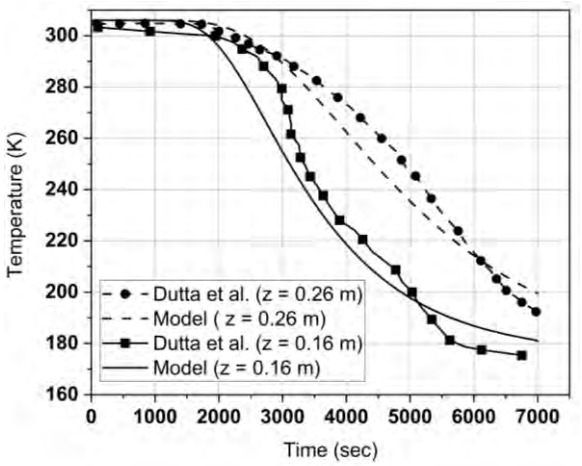

Figure 4. Temperature history at axial distance of 0.26 m and 0.16 from inlet (top)

3.2 Effect of inlet temperature on exergy losses

The effect of inlet temperature on the exergy efficiency of the charging operation was calculated and the relative contribution of each of the loss mechanism was estimated using the developed model.

3.2.1 Outlet flow exergy loss

Figure 5 shows the transient temperature distribution at the bed outlet. Due to heat transfer in the bed, a narrow thermocline region, characterized by thermal gradient started to form which separated the cold and warm part of the bed. As the bed cooled down, the thermocline region moved towards the outlet. When this thermocline started exiting the bed at t ~ 4000s, the temperature at the outlet dropped below the initial bed temperature. Consequently, the inlet exergy is lost at the outlet. With time, the rate of these exergy losses increased as the outlet temperature reached the inlet temperature.

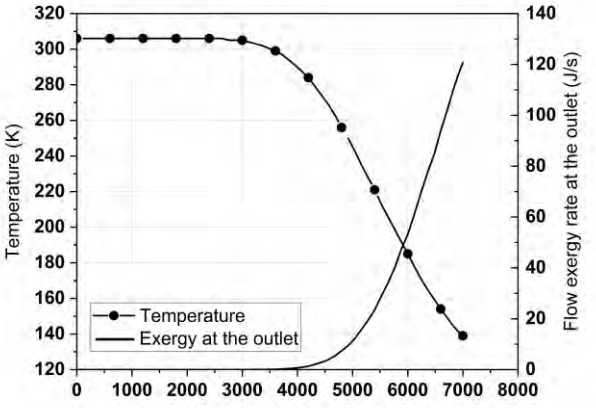

Figure 5. Transient evolution of temperature at the bed outlet (T_{in} = 100K)

Figure 6 shows various the percentage of inlet exergy loss at the outlet for different inlet temperatures. The effective thermal conductivity, which accounts for the heat exchange between packing and the gas reduced as inlet temperatures were lowered. This reduction lowered the heat transfer rate in the bed which meant that the incoming fluid left the bed without complete heat exchange. As a result, the percentage of inlet exergy losses were higher at higher temperatures.

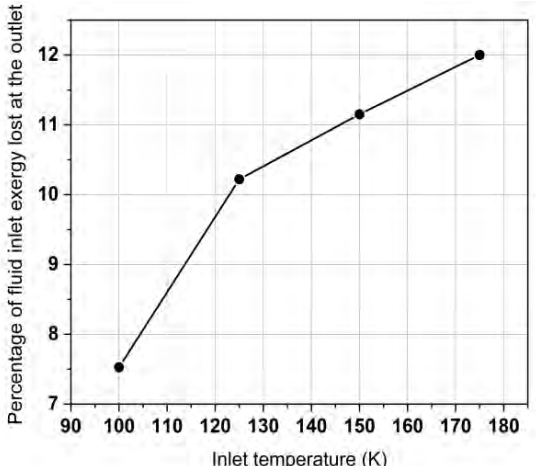

Figure 6. Percentage inlet exergy lost at the outlet

3.2.2 Axial Conduction loss

Figure 7 shows the percentage of fluid exergy lost due to axial conduction in the bed. As the inlet temperatures reduced, the driving force (difference between the initial bed temperature and the inlet temperature) for heat transfer increased which led to an increased rate of heat transfer. At the same, larger thermal gradients, i.e, steeper thermoclines were set up in the bed in the axial direction. This fact resulted in an increase in entropy generation rate which ultimately led to higher exergy losses due to conduction.

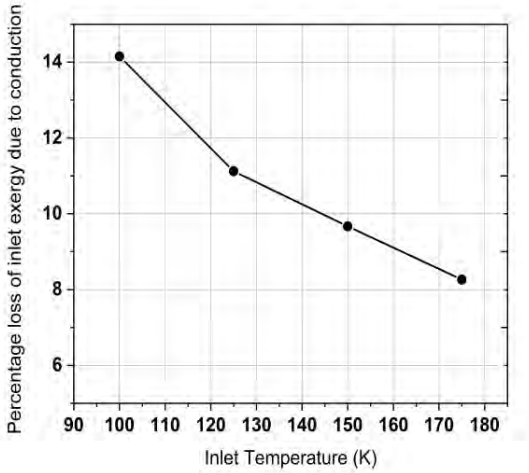

Figure 7. Percentage inlet exergy lost due to axial conduction

3.2.3 Pressure drop loss

Figure 8 shows the variation in pressure drop with inlet temperatures estimated using Ergun's equation.

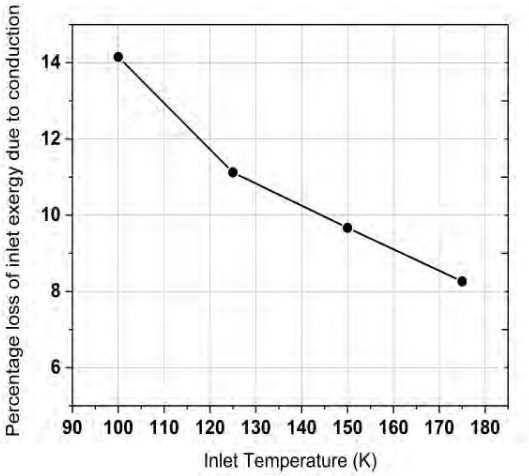

Figure 8. Pressure drops at different inlet temperatures

As the inlet temperatures increased, the gas density decreased. To maintain a constant mass flow rate, the superficial velocity reduced which lead to increase in pressure drop as temperature increased. The maximum pressure drop occurring in any of the cases (observed at 175 K and equal to 7.8 Pa) was only of the inlet pressure. Consequently, the exergy loss associated with pressure drop was found to be negligible, i.e., five orders of magnitude lower than the axial conduction losses.

3.3 Exergy efficiency of charging operation

Figure 9 shows the exergy efficiency of charging process at different inlet temperatures. Although the percentage losses at outlet dropped from 12 % to 7% when the inlet temperature was changed from 175 K to 100 K, there was a corresponding increase in percentage exergy lost due to conduction from 8.52 % to 14.2 %. The combined effect led to a drop in exergy efficiency from 79.7 % to 78% as depicted in the figure.

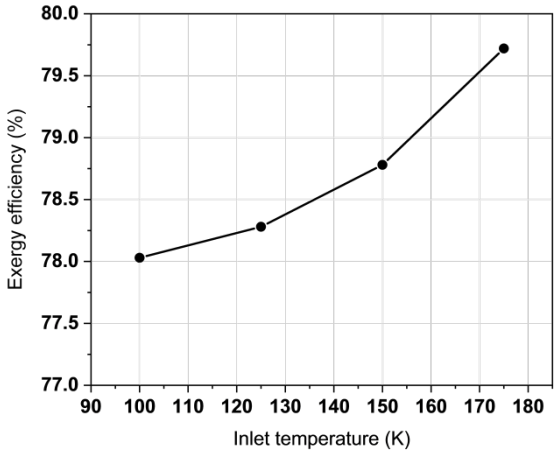

Figure 9. Effect of inlet temperature on exergy efficiency

4. CONCLUSIONS

1. Exergy loss due to pressure drop is found to be very low when compared to conduction and outlet exergy losses. Since the bed height was comparable to its diameter, axial conduction losses caused a drop in the outlet temperatures. When inlet temperatures were lowered, the axial conduction losses became dominant over

the outflow exergy losses. This caused the exergy efficiency to drop minorly as temperatures reduced.

2. To further investigate the effects of bed height, diameter, and mass flow rate, and thermophysical properties of the packing, it is essential to address certain limitations of the present model. For instance, the current one-dimensional approach did not account for ambient heat-in leaks, which could play a major role in exergy losses. Incorporating two-dimensional models would help capture the heat-in-leak effects accurately. The assumption of thermal equilibrium between fluid and packing may not hold when the thermal conductivity and volumetric heat capacity of the packing material and fluid become comparable. In such cases, a more detailed treatment of heat transfer is necessary to accurately capture the system's behaviour.

REFERENCES

1. Smith, E. M. "Storage of electrical energy using supercritical liquid air." Proceedings of the Institution of Mechanical Engineers **191**, no. 1, p.289-298, (1977)
2. Morgan, Robert, Stuart Nelmes, Emma Gibson, and Gareth Brett. "Liquid air energy storage–analysis and first results from a pilot scale demonstration plant." *Applied energy* vol. **137**, p. 845-853, (2015).
3. Sciacovelli, Adriano, Andrea Vecchi, and Yulong Ding. "Liquid air energy storage (LAES) with packed bed cold thermal storage–From component to system level performance through dynamic modelling." *Applied energy*, vol. **190**, p. 84-98, (2017).
4. Dutta Rohan, and Pavitra Sandilya. "Experimental investigations on cold recovery efficiency of packed-bed in cryogenic energy storage system." In *IOP Conference Series: Materials Science and Engineering*, vol. **755**, no. 1, p. 012103. IOP Publishing, (2020).
5. Tan Hongbo, Zhi Ding, and Na Wen. "Numerical study on the thermodynamic performance of a packed bed cryogenic energy storage system." *Applied Thermal Engineering*, vol. **214**, p. 118903. (2022).
6. Lemmon, Eric W., Marcia L. Huber, and Mark O. McLinden. "NIST reference fluid thermodynamic and transport properties–REFPROP." *NIST standard reference database* **23**, no. (2002)
7. Gonzo, Elio E. "Estimating correlations for the effective thermal conductivity of granular materials." *Chemical Engineering Journal 90*, no. **3**, p.299-302. (2002).
8. Mertens Nicolas, Falah Alobaid, Lorenz Frigge, and Bernd Epple. "Dynamic simulation of integrated rock-bed thermocline storage for concentrated solar power." *Solar Energy*, vol. **110** p. 830-842, (2014).
9. Choi Wonjun, Ryozo Ooka, and Masanori Shukuya. "Exergy analysis for unsteady-state heat conduction." *International Journal of Heat and Mass Transfer,* vol. **116**, p.1124-1142, (2018)